Fuel 150 (2015) 325–333

Contents lists available at ScienceDirect

Fuel

journal homepage: www.elsevier.com/locate/fuel

Corrosion of AISI 1020 steel in crude oil studied by the electrochemical noise measurements

Emerson C. Rios [a], Alexsandro M. Zimer [a], Paulo C.D. Mendes [a], Marcos B.J. Freitas [b], Eustáquio V.R. de Castro [b], Lucia H. Mascaro [a], Ernesto C. Pereira [a,*]

[a] Laboratório Interdisciplinar de Eletroquímica e Cerâmica (LIEC), Department of Chemistry, Federal University of São Carlos, 13565-905 São Carlos, SP, Brazil
[b] Núcleo de Competências em Química do Petróleo (NCQP), Department of Chemistry, Federal University of Espírito Santo, 29075-910 Vitória, ES, Brazil

HIGHLIGHTS

- The corrosion of steel in crude oil was studied using electrochemical noise.
- The data were treated using wavelet transform.
- The experiments were planned using factorial design.
- The effect of sea water, H_2S, naphthenic acid and immersion time were investigated.
- The approach used allowed to identify and quantify the corrosion process.

ARTICLE INFO

Article history:
Received 8 October 2014
Received in revised form 4 February 2015
Accepted 5 February 2015
Available online 20 February 2015

Keywords:
Corrosion
Crude oil
Electrochemical noise
Wavelet transform
Factorial design

ABSTRACT

In this work, the corrosion process of AISI 1020 in crude oil, to which different amounts of sea water (0.5 and 4.0% v/v), naphthenic acid (500 and 3000 ppm), and H_2S (50 and 1000 ppm) were added, was investigated using electrochemical noise at open circuit potential. The different oil samples were prepared using a 2^3 factorial design involving the three species described above. To analyze the obtained data, wavelet transform and energy distribution plot were used. Using this technique it was possible to separate the contributions of two types of corrosion, generalized and localized, in oil samples with different compositions and to analyze the effect of those variables on the changes that occurred during 55 days of immersion in the experiment. The results showed an increase in pitting formation in those steel samples studied in oil containing H_2S at 50 ppm and 4.0% sea water. The contribution of generalized corrosion on the metallic surface is higher in oil containing 3000 ppm naphthenic acid than in the other experimental conditions. The results were confirmed by morphological analysis of the corroded samples.

1. Introduction

Corrosion problems in the oil industry occur in different steps of the production and storage processes. Therefore, corrosion is an important concern when tanks, pipelines, equipment, and other steel components are used which can exhibit mechanical failures and negative environmental impacts due to it [1]. In many cases, the presence of liquid hydrocarbons can assist in its mitigation as a result of their ability to form persistent films on the metal. However, the complexity of this issue arises from the fact that crude oil has many different chemical components, such as H_2S, CO_2, naphthenic acids, and water droplets, which, together with pH, temperature, flow, and pressure changes, control the corrosion rate [2]. Of course, the cross effect of the composition and the controlling variables make the determination of the corrosion impact even more difficult.

Several methods have been proposed to study corrosion processes: mass loss, galvanic current detection, electrical resistance, and electrochemical measurements [3]. In crude oil, however, one important difficulty in using an electrochemical technique is its low ionic conductivity, which forbids continuous current experiments [4]. To overcome this problem, electrochemical impedance spectroscopy (EIS) [5–7] and electrochemical noise (ECN) [7–9] have been proposed as viable methods. In the literature [10–14], it is commonly stated that ECN is a result of changes in the surface condition of the metal, such as breakdown and repair of the surface film. Therefore, ECN provides valuable information

* Corresponding author.
E-mail address: ernesto@ufscar.br (E.C. Pereira).

http://dx.doi.org/10.1016/j.fuel.2015.02.022
0016-2361/

about complex electrochemical reactions under non-stationary conditions, which enables this method to be applied in the study of environment-assisted cracks [15–17], pitting [14,18,19], grain boundaries [19,20], and general corrosion [17,21].

ECN measurements are generally performed under open circuit conditions, E_{oc}, using two symmetric working electrodes, WE_1 and WE_2, between which the current noise signal, I_n, and the potential noise, E_n (against a pseudo-reference electrode, RE), are monitored. Under some experimental conditions the intensity and frequency noise are high, which makes the process of interpretation of ECN time series difficult. In this case, mathematical tools such as Fourier transform (FT) [11,12,21] or wavelet transform (WT) [22–24] can be used to analyze the data. WT has been proposed as an alternative tool to detect, classify, and discriminate transient signals even in the case of superposition of various physical events, with different time constants [22] from those observed in ECN experiments. Thus, it is able to overcome the limitations of FT, in which the coefficients are obtained by correlating the original signal with sine and cosine waves, which is suitable for processing stationary signals. On the other hand, WT is appropriate for the study of both stationary and non-stationary ECN time data [22]. Using WT, each component is defined by a set of wavelet coefficients that contain information about the time-scale characteristics of the associated corrosion event. Generally, WT interpretation is undertaken using energy distribution plots (EDPs) [13,19,22,25]. In this case, specifically considering corrosion data, it is possible to differentiate, both qualitatively and quantitatively, between two or more corrosion processes that are simultaneously present in the system, such as pitting and crevice corrosion [26].

Regarding the applicability of EIS and ECN techniques to study the corrosion of steel in crude oil, only a few papers have been found in the literature. Mahjani et al. [7] used these techniques to estimate the corrosion rate of carbon steel in crude oil with 20% water at room temperature and under stirring. The time series noise patterns obtained by ECN measurements were transformed into the frequency domain by fast FT and then their power spectrum densities (PSDs) at a frequency were determined for comparison with the corrosion rate. They found that the PSDs of the potential and of the current varied with changes in the electrode rotation rate and immersion time. In addition, the relationship between the corrosion rate and the spectral noise resistance was better at lower frequencies. However, information about the type of corrosion or mechanism involved has not been described. Becerra et al. [27] studied the effect of the oil content on the corrosion of AISI–SAE 1010 carbon steel in oil-in-water emulsions under controlled hydrodynamic conditions using potentiodynamic polarization and EIS. Different systems were studied including brine, surfactant solution, and oil-in-water emulsions, in which the aqueous phase was the surfactant solution and the oil phase was a mineral oil. This study found that the effect of the oil content on the electrochemical activity of carbon steel changes with the internal phase relationship (IPR). For emulsion with oil contents up to 20 wt% the electrochemical activity was slightly higher than that of the base surfactant solution. The electrochemical activity of emulsions with oil contents between 20 and 45 wt% showed almost no variation as oil content changed, while for emulsions with oil contents between 45 and 70 wt% the activity diminished. The authors explain the data in terms of a model that postulates the formation of an oily phase on the steel surface, whose stability depends on the magnitude of the hydrodynamically induced shear stress at the interface.

The crude oil composition is very complex and this fact complicates the interpretation of the results, which makes the use of experimental design and chemometric techniques very helpful. The application of chemometric techniques in the field of corrosion science is not widespread [28]. Then, considering what has been described above, in this work we study the corrosion of AISI 1020 steel in crude oil using ECN and the wavelet transform to analyze the data. Different aggressive compounds commonly encountered in oil, such as sea water, naphthenic acids, and sulfide compounds, were investigated. The approach used in this work combined with factorial design of experiments has been shown to be very useful in the detection of the main corrosive agents contained in the oil and enables a refined analysis regarding their influences on corrosion mechanisms.

2. Experimental

AISI 1020 steel (Sanchelli) was used as the working electrode. It was annealed at 900 °C for 60 min to relieve the mechanical stress and homogenize the grain size [29]. Two identical electrodes, WE_1 and WE_2, with $A = 0.7\ cm^2$ were embedded in polyester resin, side by side, separated by 0.1 cm, according to the scheme shown in Fig. 1. Prior to the tests, the working electrodes were ground to 1200 grit emery paper, and finally cleaned by acetone in an ultrasonic bath. A 1.0 cm^2 Pt plate [30] was used as the pseudo-reference RE. It was positioned parallel to the WE_1, separated by 0.1 cm, controlled by a Teflon spacer. Both potential, E_n, and current, I_n, noise were collected simultaneously.

The crude oil characteristics presented in Table 1 highlight the total water content, BSW, 0.5%. The water-in-oil emulsions were prepared by adding artificial sea water (H_2O) [31], naphthenic acid (HNap, Aldrich), and sodium sulfide (Na_2S, Synth) to the petroleum (17 °API) sample under stirring at 40 °C. In order to minimize the number of experiments to be performed, as well as to measure the cross effects among the variables, a full factorial design of three variables (concentration of H_2O, HNap, and Na_2S) at two levels was used [32,33]. In a full factorial design, n^k experiments must be performed, where n is the number of variables and k is the number of values of each one of those variables investigated. Thus, to investigate three variables at two different values each, $2^3 = 8$ experiments are needed. The eight experimental conditions

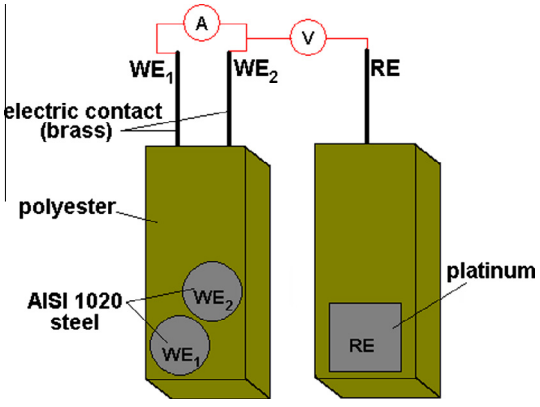

Fig. 1. Assembly of the electrodes used in this study.

Table 1
Characteristics of crude oil used in this work.

Test	Procedure	Results	Unit
Free water	Inner POP-LP-001	0.14	% v/v
BSW (emulsion–oil)	ASTM D 4007–02	0.37	% v/v
BSW total	Sum (free water + BSW)	0.51	% v/v
°API at 60 °F	Calculated	17.0	–
Salt in oil	ASTM D 6470-99	945.5	mg/L
Total acidity	ASTM D 664-06	3.25	mgKOH/g
Viscosity at 40 °C	Calculated	557.9	cSt

Table 2
Experimental matrix of the 2^3 factorial design.

Experiment	[H_2O]	[HNap]	[Na_2S]	Variables	Levels	
					(−)	(+)
01	−	−	−			
02	−	−	+			
03	−	+	−	H_2O	0.5%	4.0%
04	−	+	+			
05	+	−	−	HNap	500 ppm	3000 ppm
06	+	−	+			
07	+	+	−	Na_2S	50 ppm	1000 ppm
08	+	+	+			

investigated are presented in Table 2. The calculation of the experiments is the combination of all variables at their different values. The calculations were performed by using Calc spreadsheet program, of the LibreOffice. As response to the analysis of the effects presented in Pareto plots, the accumulated energy for each type of corrosion was used: d_1–d_4 to general corrosion and localized corrosion for d_5–d_8. To follow the aging effects of the corrosion process on the samples, the noise experiments were performed during 55 days. During this time period, the temperature of the solution was controlled at 40 °C and ECN data were collected four times, after 2, 15, 31, and 55 days.

To perform the ECN measurements at E_{oc} an Autolab-PGSTAT20 with an ECN module controlled by NOVA 1.6 software was used. The noise was registered at a sampling frequency of f_s = 6 Hz, within a period of 682 s for each record, leading to 4096 points. For stress, the maximum frequency related to a particular level in the EDP plot depends on the data acquisition rate (remember that d_1 level is the Nyquist frequency). As consequence, for purposes of comparison with other literature studies should be considered the acquisition rate of the electrochemical noise signal. The signal analysis was performed using an orthogonal Daubechies function of the fourth order, "Db4", with eight levels of decomposition. The energy distribution relative to the level coefficients, d_1–d_8, mainly reflects the information about the processes of initiation (or development) of corrosion which are under investigation. The main property of the chosen function is that the energy of the analyzed signal is equal to the sum of the energies of all components obtained by the wavelet transform; these look like fractal-type signals and a faster convergence of wavelet coefficients is therefore expected. In this work the results were interpreted by estimating the energy contribution of each level of decomposition in relation to the original signal.

To observe the corroded surface after 55 days of immersion, the samples were cleaned with pure gasoline and toluene in an ultrasonic bath, and then analyzed using optical microscopy. The Image-J software was used to analyze of the images obtained.

3. Results and discussion

The system under investigation has a slow approach towards the steady state, and therefore it was left to rest for two days before performing the first measurement. After that period of immersion, the potential and current noise had intensities of 10^{-5} V and 10^{-9} A, respectively. Although the ECN technique allows the acquisition of both signals (E and I), only the current noise was analyzed. Abrupt changes in the potential and/or current are related to the local disruption of the passive layer, which is followed by repassivation, leading once again to an increase in E_n and decrease in I_n. In most cases, the reduction reaction is not fast enough to consume all the species coming from metal oxidation, causing the majority of the charge generated to be used for recharging of the capacitive film [34]. Thus, the slow recovery of potential transients is caused by the capacitive discharge process, while current transients reflect initiation, growth, and repassivation processes of pitting. Therefore, it is convenient to use only the I_n signal for the quantitative analysis of the corrosion process.

Fig. 2 shows the I_n signal measured using the setup described above for the different experimental conditions described in Table 2. First, different qualitative aspects of the noise patterns can be discussed. For example, in this figure it is possible to observe that for the samples containing 0.5% v/v seawater (experiments 01–04) the intensity I_n is lower than for the samples containing 4.0% v/v (experiments 05–08).

Under the experimental conditions, when corrosion occurs, the anodic current flow is consumed by: (i) double layer charging, (ii) dissolution of the passive layer formed on the metal surface, and/or (iii) faradaic reactions at the metal/oil interface. Different papers [35–40] have proposed that high intensity noise is related to pit formation, and it is common sense that the adsorption of aggressive ions such as chloride is necessary for their initiation. When the Cl^- concentration was increased (experiments 05–08), an increase in the number of current transients was observed. In the literature [36] these are described as being associated with the aggressiveness of Cl^- ions over the passive film. At this point, it is important to stress that the current scales in Fig. 2 are different. To make this point clear, an inset of experiment 06 using the same scale as experiment 02 is also presented in this figure.

Fig. 3 shows I_n for different immersion times: 2 and 55 days of immersion. In this figure, it was necessary to use a different amplitude scale to highlight the current noise data. First, it is important to observe that an apparent change in the noise pattern occurred as the immersion time increased. From a direct visual inspection, it is also possible to appreciate that the time-scale of the fluctuations observed in two days is smaller than that observed in 55 days. This difference can be linked to a change in the corrosion mechanism, as when the immersion time increases the thickness and stoichiometric composition of the film formed could change. As described in the Introduction, an increase in the current amplitude transient could be associated with an increase in the pit formation process [8]. Then, from Fig. 3, it is possible to propose that after 55 days the pit corrosion has an important effect on the corrosion of steel here investigated. This can be confirmed by the optical micrographs also shown in Fig. 3, where there are a greater number of localized attacks after 55 days of immersion compared to 2 days.

In conclusion, even a qualitative analysis is very complex for the data presented in Figs. 2 and 3. For a detailed analysis, it is necessary to set up a method to detect and to quantify such changes which would have a direct utility for monitoring the corrosion. In other words, it is not simple to assign changes in the type or corrosion rate using the ECN in the time domain, since the transients can overlap each other during simultaneous formation of two (or more) pits, leading to convoluted oscillations that can be incorrectly interpreted as multiple transients.

Several methods of converting time domain data can be used, making it possible to obtain quantitative and qualitative information. Among these methods are FT and WT, as described in the Introduction of this paper along with the advantages of the latter mathematical procedure. Therefore, in order to separate the contributions of the processes, the WT was applied to all current noise data. These signals are composed of different events that can be classified according to their frequency. The schematic diagram for the WT used to analyze the data is shown in Fig. 4, where the relationship of the frequency of each level of decomposition (d_1–d_8) with the number of data, which is halved in every stage of decomposition, is illustrated. The Daubechies wavelet was chosen since it presents a similar shape to the current noise signal obtained here. Whereas the intensity and frequency noise are related to the type of corrosion, it is possible to associate and quan-

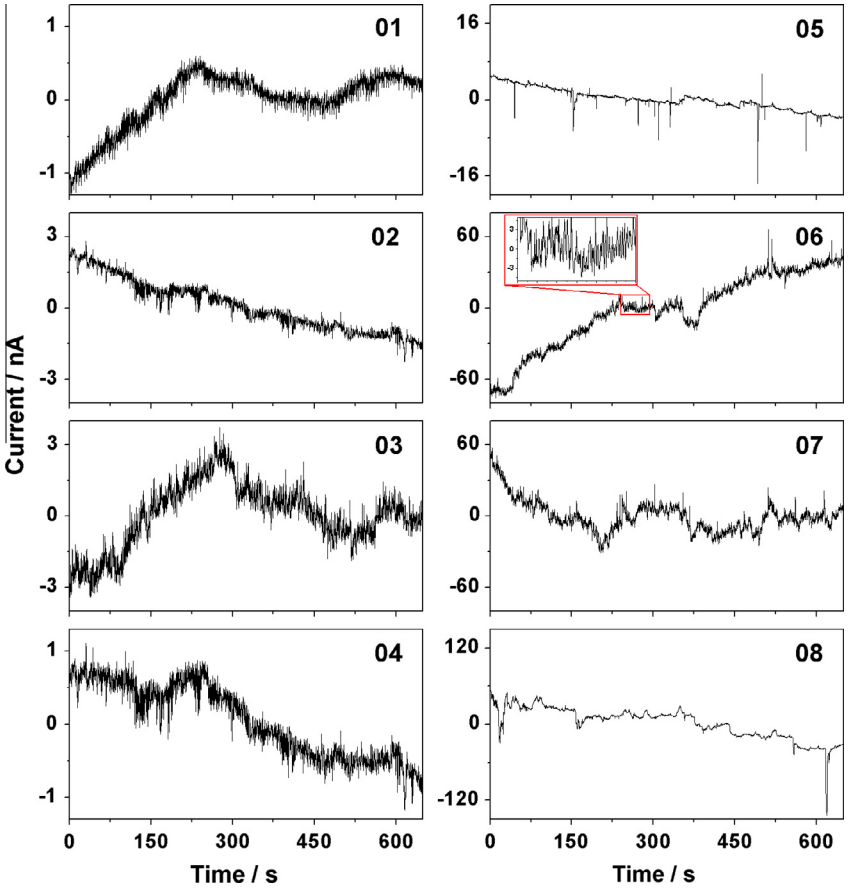

Fig. 2. Current noise of AISI 1020 in oil samples with different compositions (described in Table 2) after 48 h of immersion, (T = 40 °C).

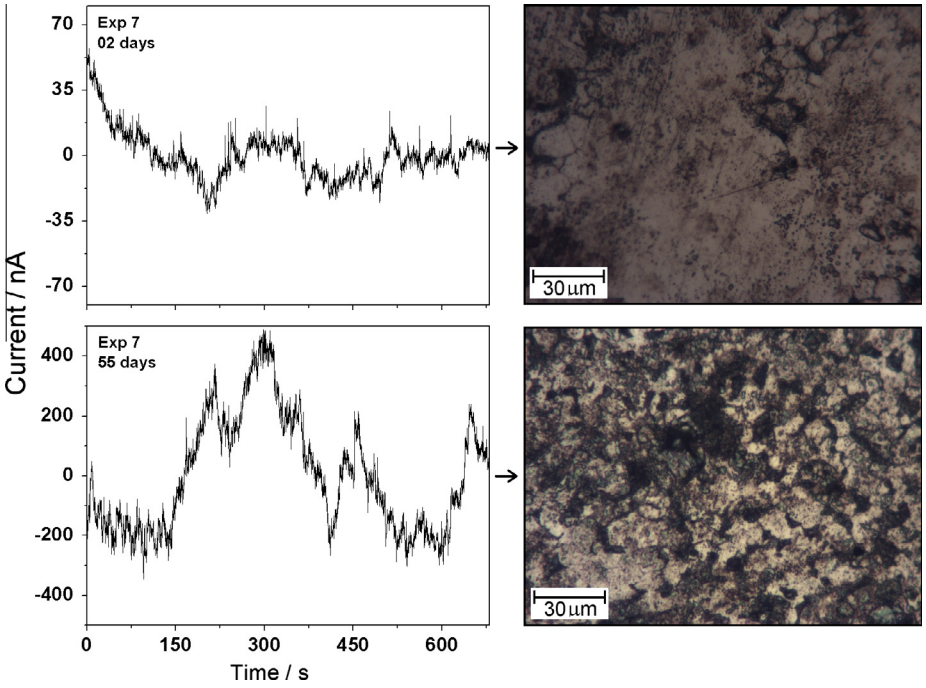

Fig. 3. Current noise of AISI 1020 carbon steel in crude oil with composition of experiment 07 (Table 1) after 2 and 55 days of immersion, and optical micrographs in the respective immersion times, (T = 40 °C).

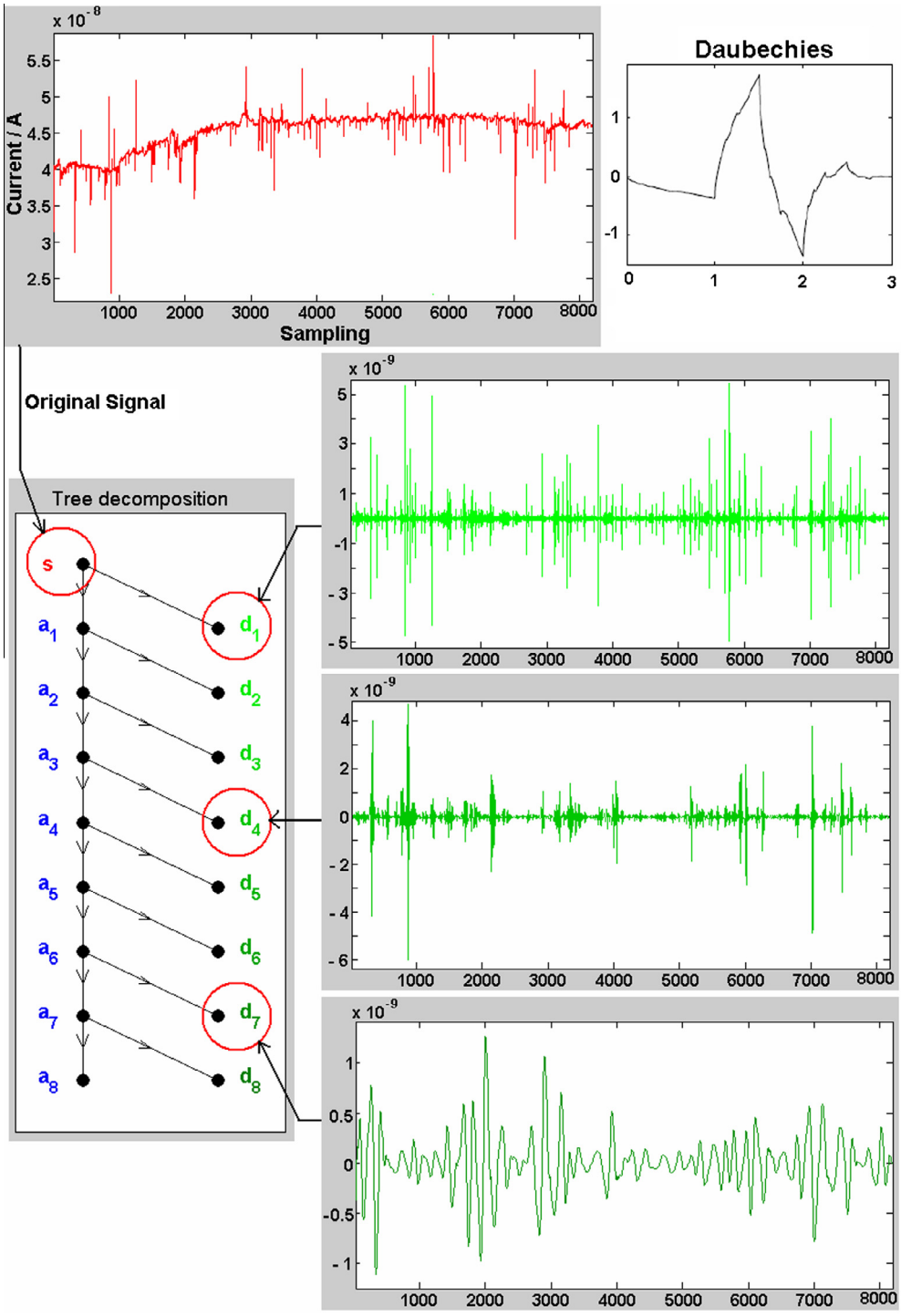

Fig. 4. Diagram of energy decomposition of the ECN signal current through the wavelet transform.

tify the energy accumulated in each decomposition level relating to the type of corrosion with the original current signal through energy distribution plots (EDPs). Then, using such transforms in the context of the frequency domain clarifies those variations in the profile of the current noise, making it possible to correlate the characteristic patterns of the signal with the chemical–physical phenomena [22–24].

The EDPs relative to the level coefficients, d_1–d_8, mainly reflect information concerning the processes of initiation (or development) of corrosion being investigated. Several studies [12–14,18,38,41,42] have shown that current transients related to the localized process, such as pitting, has lifetime higher than 2 s (frequency < 0.5 Hz). Therefore, this feature of the lifetime of the current transient places the localized processes in low frequency levels (d_5–d_8) in the EDP plots. The total time of transient oscillation is related with a pit formation, and the stages of growth and pit repassivation last longer than the transient current. Therefore, we can correlate the most part of the charge consumed during process with the steps which last a longer period of time. Otherwise, in some cases, it was described in the literature [22,43] that the initial current transient pulse

related to a pitting (narrow spike) formation can also be contained in the high frequency levels. However, even in these cases, most part of the energy appears during the slow decay of the transient and is associated with low frequency levels.

Taking these aspects into account, in the present paper the levels d_1–d_4 ($f > 0.38$ Hz) could be attributed to general corrosion, while the remaining levels, d_5–d_8, could be associated with localized corrosion processes ($f < 0.38$ Hz) such as pit formation. Fig. 5 presents the energy dispersion for the different levels of decomposition obtained by the WT applied to the ECN data of experiments listed in Table 2 over 55 days. As can be observed in Fig. 5, there are important changes in the energy dispersion levels of both intervals, d_1–d_4 and d_5–d_8, as the period of immersion increases, which could be related to changes in the corrosion rate or mechanism or both.

Analyzing the signal decomposition presented in Fig. 5, an enhancement of localized corrosion can be proposed for most of the cases, as well as a consequent decrease in the contribution of the generalized process as the period of immersion increases. One possible explanation for such a change could be that in the initial stage, formation of the mackinawite species occurs ($Fe_{(1+x)}S$, $x = 0$–0.125); this species is unstable and is inter-converted into iron monosulfide (FeS) [44]. After some time, however, the FeS film could dissolve, exposing the metal again [45]. In this initial period, the film growth and redissolution process lead to a generalized corrosion behavior [34,40,46]. At the end of the experiment, it was observed that the localized corrosion had become the main contribution of the signal.

To support the results obtained by ECN analysis, images were obtained using optical microscopy after 55 days of immersion under the experimental conditions studied. The micrographs presented in Fig. 6 show the presence of two types of corrosion. However, the contribution of energy in the processes of generalized and localized corrosion is different in each case, as concluded above from wavelet analysis. The corroded region is distinguished by darker tone compared to not corroded region. Thus, it is possible to compare via the same threshold of the grayscale (from image in 8 bits) the intensity of attacks among different images. For the samples investigated using the experimental conditions of experiments 02 and 06 (Table 2) it is possible to observe the existence of two types of corrosion. After 55 days of immersion, analyzing the data in the energy distribution plots in Fig. 5 for sample 02 and 06, it is possible to conclude that generalized corrosion contribute to 26% and 10% of the total corrosion, respectively. This conclusion is corroborated from the images for sample 02 and 06 showed in Fig. 6a and b, respectively, it is clear that the main corrosion process for sample 02 is generalized whereas, for sample 06, the presence of generalized corrosion is less evident.

In order to correlate the effects of the three corrosive species with the types of corrosion during the experiments a factorial design approach was used. Fig. 7 shows the normalized Pareto plots [32] used to interpret these effects. As a response, the sum of the dispersion energy related to the generalized process was chosen, that is, levels d_1–d_4. Then, if the effect is higher than zero, the generalized corrosion is mainly observed under those conditions. Otherwise, if an effect has a negative value (to the left of the central axis) it means that there is an important contribution of the localized corrosion. The effect of the immersion period is also investigated and is presented in Fig. 7 for 2, 15, 31, and 55 days. Finally, the two vertical dotted lines are the limits of the experimental significance; that is, if the effect value is between these limits, it is below the experimental error.

Analyzing the data shown in Fig. 7, it is possible to conclude that at the beginning of the process (two days) the most important effect that influences the existence of localized corrosion is the sea water concentration, followed by the sulfide concentration (variables 1 and 3 of Table 2). The corrosive effect of sea water on a fresh steel surface is expected since the inclusions and grain boundaries are very sensitive to attack by chloride ions. Besides, it is well established in the literature [46,47] that sulfide ions make the situation concerning the localized corrosion even worse. From

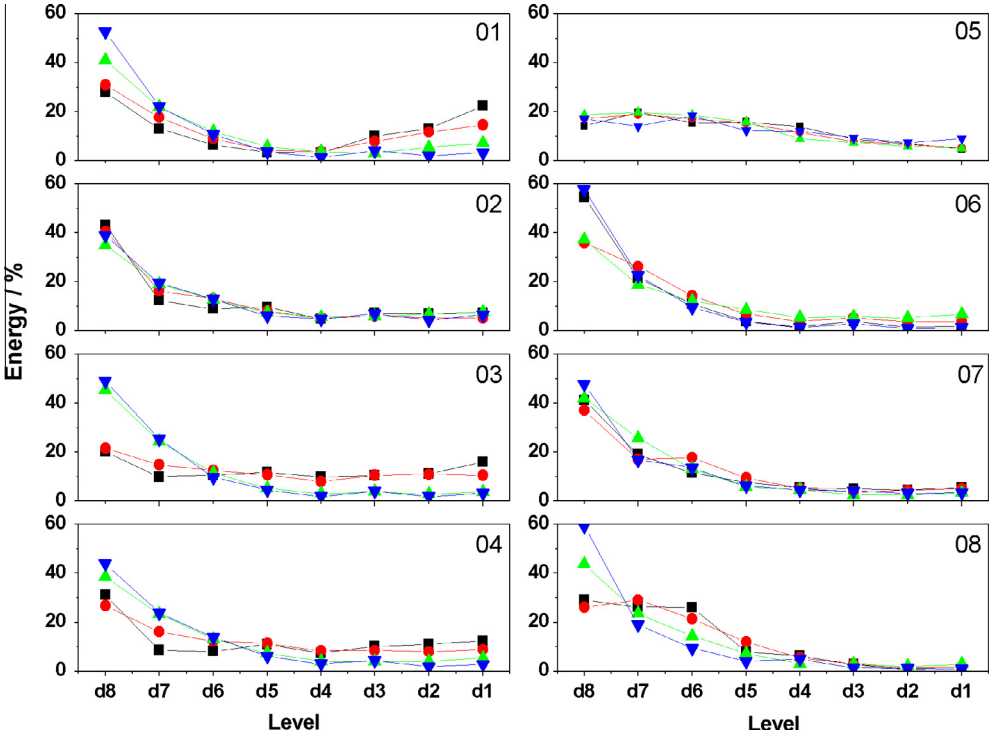

Fig. 5. Energy distribution plot (EDP) of the steel/oil system in experimental conditions (Table 2) after different days of immersion: (■) 2 days, (●) 15 days, (▲) 31 days, (▼) 55 days. (For interpretation of the references to colors in this figure legend, the reader is referred to the web version of this paper.)

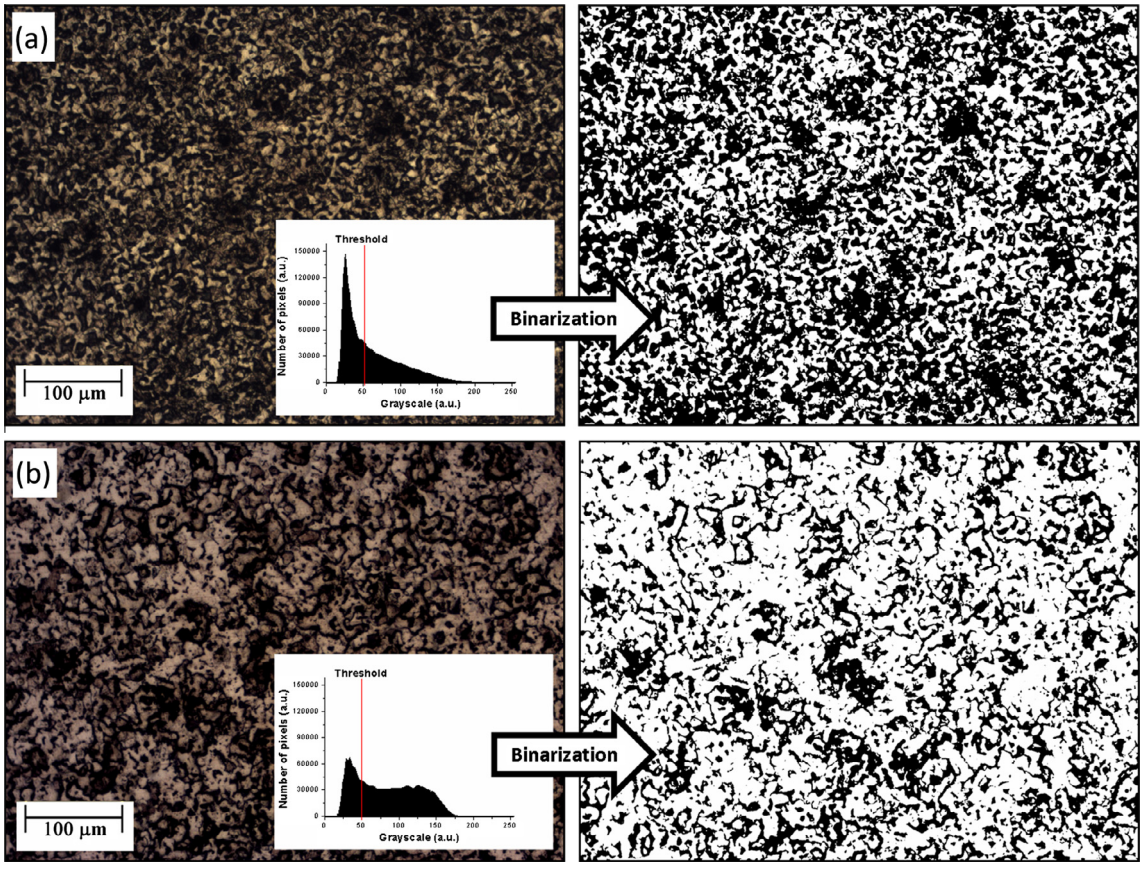

Fig. 6. Optical micrographs of AISI 1020 steel after 55 days of immersion in oil at 40 °C. (a) Exp. 02: 0.5% H_2O; 500 ppm HNap; 1000 ppm Na_2S and (b) Exp. 06: 4.0% H_2O; 3000 ppm HNap; 1000 ppm Na_2S.

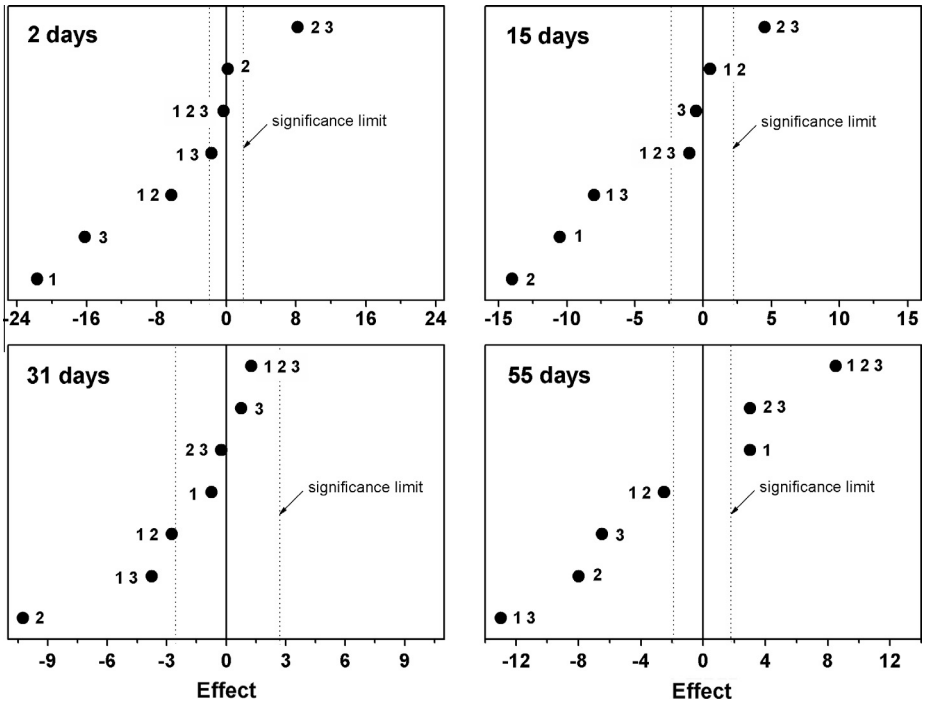

Fig. 7. Normalized Pareto plots to interpret the calculated effects using the experiments presented in Table 1. The response used was summation of levels d_1–d_4 of dispersion energy obtained by wavelet transform analysis. Variables: (1) sea water, (2) naphthenic acid, (3) Na_2S.

a different point of view, the cross effect between the naphthenic acid and sulfide ions (variables 2 and 3 of Table 2), which leads to the predominance of generalized corrosion, could be attributed to the ability of some organic acids to redissolve the FeS film formed on the ferritic grains [45,46].

For those experiments in which measurements were conducted at intermediate immersion time periods, 15 and 31 days, a continuous change in the effect values can be observed in Fig. 7. Finally, after 55 days of immersion, a description of the effect of the different variables is more complicated. Now, the effect of sea water is mainly related to the generalized corrosion. This could be explained by considering that different products of corrosion are on the surface and could contribute to modifying the effect of the most aggressive species in sea water: chloride ions. Indeed, after 55 days of immersion, the cross effect of the three variables is one of the most important and contributes mainly to the generalized corrosion. This cross effect could be related to the fact that the inclusions, which were active during pit nucleation, are no longer important. On the other hand, the effects of naphthenic acid and sulfide ions (variables 2 and 3 of Table 2) are also related to the generalized corrosion. According Yépez [46], when the oxidizing agent is H_2S, FeS film forms, which decreases the aggressive effect of the naphthenic acid. However, if the oxidizing agent is H_2O, further dissociation of the naphthenic acid could occur and then the cathodic reaction rate would increase, leading to an overall corrosive aggressive effect of the naphthenic acid. In conclusion, the set of experiments used in this work demonstrates the possibility of detecting various corrosion processes encoded in a complex signal, as in the case of ECN. Furthermore, it was possible to evaluate the relative weights of the two processes occurring simultaneously.

4. Conclusions

The results showed an increase in pitting formation in those steel samples studied in the oil containing H_2S at 50 ppm and 4.0% sea water. The contribution of generalized corrosion on the metallic surface was higher in the oil sample containing 3000 ppm naphthenic acid than in the other experimental conditions. It was also possible to observe the importance of the different variable changes as the period of immersion increased. It is possible to conclude that for short exposition times (two days) the most important effect that influences the localized corrosion is the sea water concentration, followed by the sulfide concentration. Besides, the cross effect between the naphthenic acid and sulfide ions, which can only be calculated using a factorial design, leads to the predominance of generalized corrosion. After 55 days of immersion, the cross effect of the three variables is one of the most important and contributes mainly to the generalized corrosion together with the effect of sea water, which initially contribute to the localized corrosion.

The combined use of the electrochemical noise technique, wavelet transform analysis, and the chemometric approach allowed us to qualify and quantify corrosion in a steel/oil environment. The methodology used in this work demonstrates the possibility of detecting and assessing the relative contributions of different corrosion processes (localized and generalized) occurring at the same time in a complex system. Consequently, signal processing analyzes of this kind can be an efficient tool for corrosion monitoring in the oil industry.

Acknowledgements

The authors would like to thank FAPESP (Proc.: 98/14324-0, 2011/19430-0, 2013/26233-1), CNPq, and CAPES for financial support.

References

[1] Restrepo CE, Simonoff JS, Zimmerman R. Causes, cost consequences, and risk implications of accidents in US hazardous liquid pipeline infrastructure. Int J Crit Infrastruct Prot 2009;2:38–50.
[2] Soares CG, Garbatov Y, Zayed A, Wang G. Corrosion wastage model for ship crude oil tanks. Corros Sci 2008;50:3095–106.
[3] Yang L. Techniques for corrosion monitoring. Cambridge (England): CRC Press; 2008.
[4] Hack HP, Moran PJ, Scully JR. The measurement and correction of electrolyte resistance in electrochemical tests. Cambridge (England): ASTM STP 1056; 1990.
[5] Goual L. Impedance spectroscopy of petroleum fluids at low frequency. Energy Fuel 2009;23:2090–4.
[6] Lvovich VF, Smiechowski MF. Impedance characterization of industrial lubricants. Electrochim Acta 2006;51:1487–96.
[7] Mahjani MG, Neshati J, Masiha HP, Jafarian M. Electrochemical noise analysis for estimation of corrosion rate of carbon steel in crude oil. Anti-Corros Method Mater 2007;54:27–33.
[8] Dawson JL. Electrochemical noise measurement for corrosion applications. ASTM STP 1277; 1999.
[9] Tan Y. Experimental methods designed for measuring corrosion in highly resistive and inhomogeneous media. Corros Sci 2011;53:1145–55.
[10] Hashimoto M, Miyajima S, Murata T. A stochastic analysis of potential fluctuation during passive film breakdown and repair on iron. Corros Sci 1992;33:885–904.
[11] Shi Z, Song G, Cao C, Lin H, Lu M. Electrochemical potential noise of 321 stainless steel stressed under constant strain rate testing conditions. Electrochim Acta 2007;52:2123–33.
[12] Cheng YF, Luo JL, Wilmott M. Spectral analysis of electrochemical noise with different transient shapes. Electrochim Acta 2000;45:1763–71.
[13] Qiao G, Ou J. Corrosion monitoring of reinforcing steel in cement mortar by EIS and ENA. Electrochim Acta 2007;52:8008–19.
[14] Dong ZH, Shi W, Guo XP. Initiation and repassivation of pitting corrosion of carbon steel in carbonated concrete pore solution. Corros Sci 2011;53:1322–30.
[15] Acuña-González N, García-Ochoa E, González-Sánchez J. Assessment of the dynamics of corrosion fatigue crack initiation applying recurrence plots to the analysis of electrochemical noise data. Int J Fatigue 2008; 30:1211–9.
[16] Gomez-Duran M, Macdonald DD. Stress corrosion cracking of sensitized Type 304 stainless steel in thiosulphate solution. II. Dynamics of fracture. Corros Sci 2006;48:1608–22.
[17] Edgemon GL, Danielson MJ, Bell GEC. Detection of stress corrosion cracking and general corrosion of mild steel in simulated defense nuclear waste solutions using electrochemical noise analysis. J Nucl Mater 1997;245:201–9.
[18] Kiwilszo M, Smulko J. Pitting corrosion characterization by electrochemical noise measurements on asymmetric electrodes. J Solid State Electr 2009;13:1681–6.
[19] Cao FH, Zhang Z, Su JX, Shi YY, Zhang JQ. Electrochemical noise analysis of LY12-T3 in EXCO solution by discrete wavelet transform technique. Electrochim Acta 2006;51:1359–64.
[20] Pujar MG, Parvathavarthini N, Dayal RK, Thirunavukkarasu S. Assessment of intergranular corrosion (IGC) in 316(N) stainless steel using electrochemical noise (EN) technique. Corros Sci 2009;51:1707–13.
[21] Girija S, Mudali UK, Raju VR, Dayal RK, Khatak HS, Raj B. Influence of stacking fault energy on nanostructure formation under high pressure torsion. Mat Sci Eng A-Struct 2005;40:7188–95.
[22] Aballe A, Bethencourt M, Botana F, Marcos M. Using wavelets transform in the analysis of electrochemical noise data. Electrochim Acta 1999; 44:4805–16.
[23] Dong Z, Guo X, Zheng J, Xu L. Calculation of noise resistance by use of the discrete wavelets transform. Electrochem Commun 2001;10:561–5.
[24] Planinsic P, Petek A. Characterization of corrosion processes by current noise wavelet-based fractal and correlation analysis. Electrochim Acta 2008;53:5206–14.
[25] Zhao B, Li JH, Hu RG, Du RG, Lin CJ. Study on the corrosion behavior of reinforcing steel in cement mortar by electrochemical noise measurements. Electrochim Acta 2007;52:3976–84.
[26] Dai XD, Motard RL, Joseph B, Silverman DC. Corrosion process monitoring using wavelet analysis. Ind Eng Chem Res 2000;39:1256–63.
[27] Becerra HQ, Retamoso C, Macdonald DD. The corrosion of carbon steel in oil-in-water emulsions under controlled hydrodynamic conditions. Corros Sci 2000;42:561–75.
[28] Luciano G, Traverso P, Letardi P. Applications of chemometric tools in corrosion studies. Corros Sci 2010;52:2750–7.
[29] Machado IF. Technological advances in steels heat treatment. J Mater Process Technol 2006;172:169–73.
[30] Freitas R, Oliveira R, Santos M, Bulhões L, Pereira E. Preparation of Pt thin film electrodes using the Pechini method. Mater Lett 2006;60:1906–10.
[31] Lyman J, Fleming RH. Composition of seawater. J Mar Res 1940;3:134–46.
[32] Neto BB, Scarminio I, Bruns R. Statistical design – chemometrics. Elsevier Science; 2006.
[33] Torbjorn L, Elisabeth S, Lisbeth A, Bernt T, Asa N, Jarle P, et al. Experimental design and optimization. Chemom Intell Lab Syst 1998;42:3–40.

[34] Cheng Y. Analysis of the role of electrode capacitance on the initiation of pits for A516 carbon steel by electrochemical noise measurements. Corros Sci 1999;41:1245–56.
[35] Organ L, Scully JR, Mikhailov AS, Hudson JL. A spatiotemporal model of interactions among metastable pits and the transition to pitting corrosion. Electrochim Acta 2005;51:225–41.
[36] Cheng Y, Wilmott M, Luo J. The role of chloride ions in pitting of carbon steel studied by the statistical analysis of electrochemical noise. Appl Surf Sci 1999;152:161–8.
[37] Berthomé G, Malki B, Baroux B. Pitting transients analysis of stainless steels at the open circuit potential. Corros Sci 2006;48:2432–41.
[38] Punckt C, Bölscher M, Rotermund HH, Mikhailov AS, Organ L, Budiansky N, et al. Sudden onset of pitting corrosion on stainless steel as a critical phenomenon. Science 2004;305:1133–6.
[39] Wang H, Xie J, Yan K, Duan M, Zuo Y. The nucleation and growth of metastable pitting on pure iron. Corros Sci 2009;51:181–5.
[40] Scully JR, Budiansky ND, Tiwary Y, Mikhailov AS, Hudson JL. An alternate explanation for the abrupt current increase at the pitting potential. Corros Sci 2008;50:316–24.
[41] Tian Wenming, Dub Nan, Li Songmei, Chen Sibing, Qunying W. Metastable pitting corrosion of 304 stainless steel in 3.5% NaCl solution. Corros Sci 2014;85:372–9.
[42] Soltis J, Krouse DP, Laycock NJ, Zavadil KR. Automated processing of electrochemical current noise in the time domain: I. Simulated signal. Corros Sci 2010;52:838–47.
[43] Smulko J, Darowicki K, Zielinski A. Detection of random transients caused by pitting corrosion. Electrochim Acta 2002;47:1297–303.
[44] Arzola S, Genesca J. The effect of H_2S concentration on the corrosion behavior of API 5L X-70 steel. J Solid State Electr 2005;9:197–200.
[45] Zimer AM, Rios EC, Mendes PCD, Gonçalves WN, Bruno OM, Pereira EC, et al. Investigation of AISI 1040 steel corrosion in H_2S solution containing chloride ions by digital image processing coupled with electrochemical techniques. Corros Sci 2011;53:3193–201.
[46] Yépez O. Influence of different sulfur compounds on corrosion due to naphthenic acid. Fuel 2005;84:97–104.
[47] Laredo GC, López CR, Álvarez RE, Cano JL. Naphthenic acids, total acid number and sulfur content profile characterization in Isthmus and Maya crude oils. Fuel 2004;83:1689–95.